Supplemental Tables and Figures for

Nucleotide Levels Regulate Germline Proliferation through Modulating GLP-1/Notch Signalling in *C. elegans*

Congwu Chi, Diana Ronai, Minh T. Than, Cierra J. Walker, Aileen K. Sewell and Min Han

Howard Hughes Medical Institute and Department of Molecular, Cellular & Developmental Biology, University of Colorado at Boulder, Boulder, CO 80309, USA.

Supplemental Table

Feeding bacteria/supplement	% Viable *pyr-1(lf)* animals (n)
OP50	6.5 (1939)
HT115	50.6 (1652)
OP50/*cytR*$^-$	29.3 (2530)
OP50+Uridine	33.5 (1878)

Table S1, related to Fig. 1. Feeding *cytR*$^-$ *E. coli* suppresses the lethality of worms defective in *de novo* pyrimidine synthesis, further supporting that *cytR- E. coli* serves as a uridine-rich diet for worms. Analysis of *pyr-1(cu8)* embryonic viability under different feeding conditions. "n": total eggs/worms counted in each condition. To further confirm that the *cytR*$^-$ *E. coli* strain provides more uridine, we analyzed a mutant worm strain with a *lf* mutation in the *pyr-1* gene that encodes a key enzyme in *de novo* pyrimidine synthesis (Franks et al. 2006). *pyr-1(lf)* worms fed OP50 *E. coli* display a highly penetrant embryonic lethality that is significantly suppressed by uridine supplementation (Franks et al. 2006). We found that feeding *pyr-1(lf)* worms with bacteria carrying the *cytR*$^-$ mutation (either OP50/*cytR*$^-$ or the HT115 strain commonly used for feeding-RNAi) restored the viability of *pyr-1(lf)* embryos to a similar extent as uridine supplementation.

Supplemental Figures

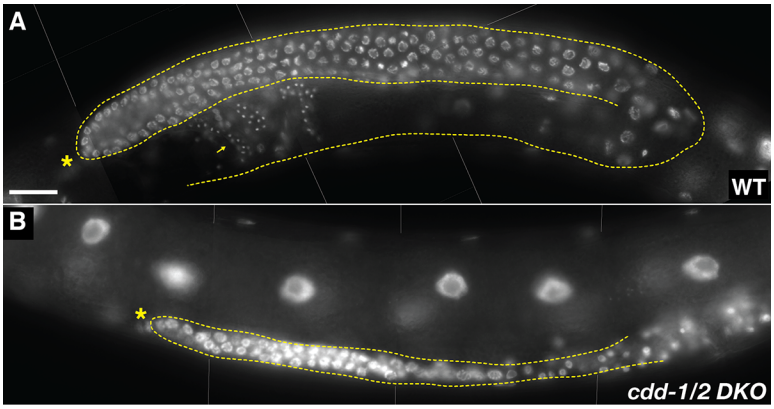

Supplemental Fig. S1, related to Table 1. Deficiency of the *rnc* gene in *E. coli* is not responsible for the rescue of fertility of *cdd-1/2* DKO worms by feeding the HT115 *E. coli* strain.

(A and B) DAPI stained images of young adult hermaphrodites of indicated genotypes fed OP50/*rnc*$^{-}$ *E. coli*. As shown in Table 1, *cdd-1/2* DKO worms fed OP50/*rnc*$^{-}$ bacteria is 100% sterile compared to 100% fertile in wild type fed the same food. Asterisk marks the distal end of gonad; dashed line outlines germline and the somatic gonadal cells; arrow marks the mature sperms. Scale bar, 20μm.

Description of the test: HT115 is widely used for feeding RNAi in *C. elegans* primarily because it is RNase III defective (*rnc*$^{-}$). To test whether *rnc*$^{-}$ is responsible for the rescuing effect observed with HT115 *E. coli*, a mutated OP50 strain was generated by replacing the wild-type copy of *rnc* with a kanamycin-resistance gene using the recombineering technique (Sharan et al. 2009). No rescue of the fertility was observed when *cdd-1/2* DKO worms were fed this OP50/*rnc*$^{-}$ bacteria as shown in (B), suggesting additional unidentified mutation(s) in the HT115 genome may be responsible for the fertility restoration of *cdd-1/2* DKO worms.

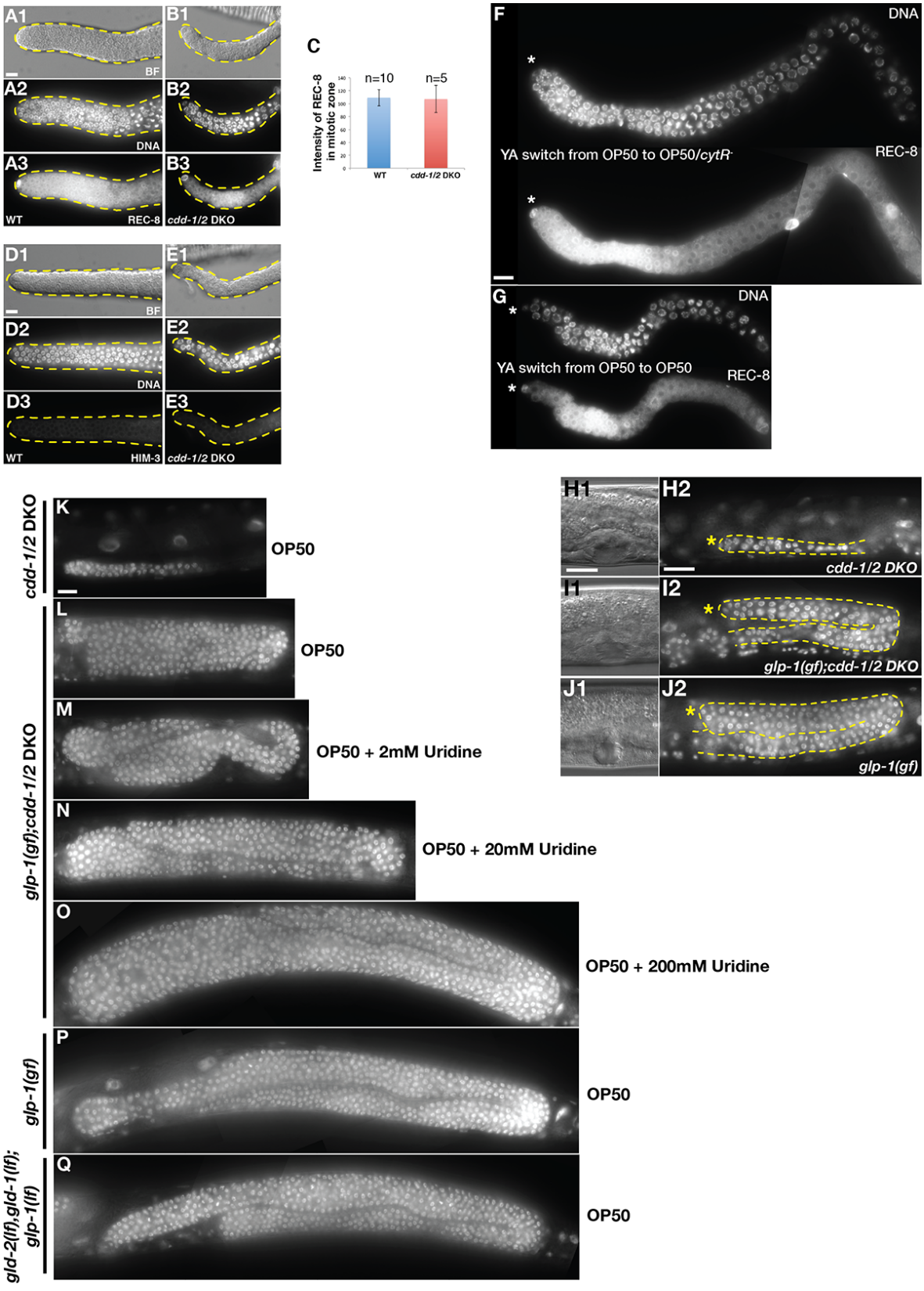
A1
B1
BF
A2
B2
DNA
A3
B3
WT
REC-8
cdd-1/2 DKO
C
Intensity of REC-8 in mitotic zone
n=10
n=5
WT
cdd-1/2 DKO
D1
E1
BF
D2
E2
DNA
D3
E3
WT
HIM-3
cdd-1/2 DKO
F
DNA
YA switch from OP50 to OP50/cytR-
REC-8
G
DNA
YA switch from OP50 to OP50
REC-8
H1
H2
cdd-1/2 DKO
I1
I2
glp-1(gf);cdd-1/2 DKO
J1
J2
glp-1(gf)
cdd-1/2 DKO
K
OP50
glp-1(gf);cdd-1/2 DKO
L
OP50
M
OP50 + 2mM Uridine
N
OP50 + 20mM Uridine
O
OP50 + 200mM Uridine
glp-1(gf)
P
OP50
gld-2(lf),gld-1(lf); glp-1(lf)
Q
OP50

Supplemental Fig. S2, related to Fig. 3. Analysis of mitotic proliferation arrests in *cdd-1/2* DKO worms.

(A-E) Characterization of undifferentiated mitotic cells in the distal gonad region.
(A and B) Representative bright field (BF, top), DAPI staining (DNA, middle) and anti-REC-8 staining (REC-8, bottom) images of dissected gonads from worms of indicated genotypes. Scale bar, 5μm.
(C) Pixel intensity quantification of anti-REC-8 staining within the whole mitotic zone of worms with indicated genotypes. n= total number of gonad arms examined in each group.
(D and E) Representative bright field (BF, top), DAPI staining (DNA, middle) and anti-HIM-3 staining (HIM-3, bottom) images of dissected gonads from worms of indicated genotypes. Scale bar, 5μm.
(F and G) Mitotic cell proliferation in *cdd-1/2* DKO germline is significantly recovered when the U/T availability is restored by food switch. Representative DAPI staining (DNA) and anti-REC-8 staining (REC-8) images of dissected gonads from *cdd-1/2* DKO worms of indicated food switching condition. Scale bar, 5μm. Young adults (YA) were switched from U/T-poor food (OP50) to either U/T-rich (OP50/*cytR*$^{-}$) or U/T-poor food (OP50) for 24 hours. Statistical data is presented in Fig. 3C.
(H-J) Effective suppression of the germline proliferation arrest of *cdd-1/2* DKO worms by *glp-1(gf)* at L4 stage. DIC (left) and DAPI staining (right) images of representative L4 stage worms of indicated genotypes. The L4 stage was determined by the morphology of the vulva of each worm under DIC (left). Statistical data of the total number of germline cells are shown in Fig. 3I. Asterisk marks the distal end of gonad; dashed line outlines germline in (right). Scale bar, 20μm.
(K-Q) Dosage dependent effect of uridine supplement on the germline size in the *glp-1(gf);cdd-1/2 DKO* triple mutant. DAPI stained images of the gonad from representative young adult hermaphrodites of indicated genotypes. The feeding condition is indicated to the right of each image. Scale bar, 20μm.

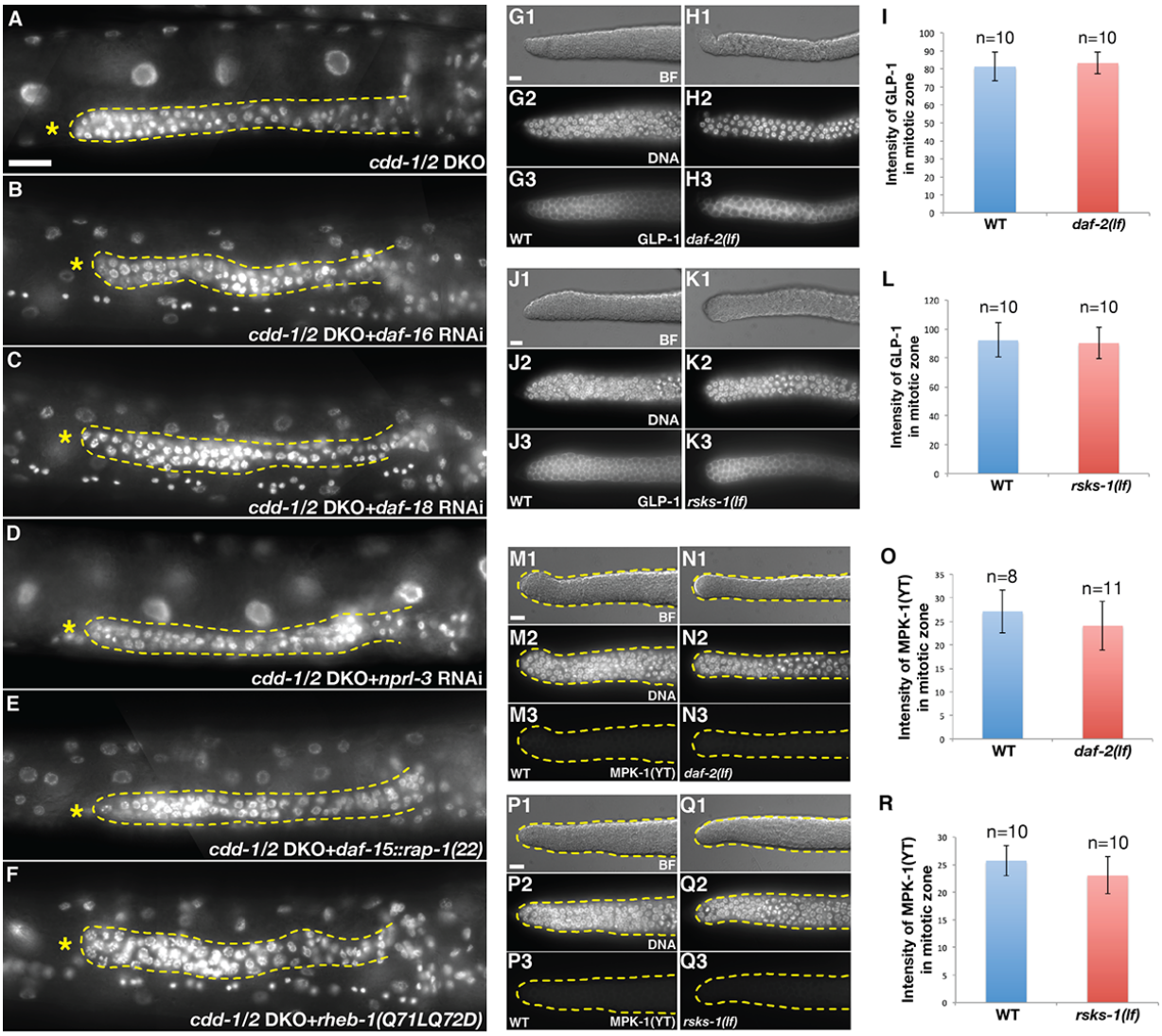

Supplemental Fig. S3, related to Fig. 3-5. Neither the IIS nor TORC1 pathways are likely to play major roles in mediating the impact of low U/T level on mitotic germline proliferation in the *cdd-1/2* DKO.

(A-F) DAPI stained images of young adult hermaphrodites of indicated genotypes. Asterisk marks the distal end of gonad; dashed line outlines germline. Scale bar, 20μm.

(G-H, J-K) Representative bright field (BF, top), DAPI staining (DNA, middle) and anti-GLP-1 staining (GLP-1, bottom) images of dissected gonads from worms of indicated genotypes. Scale bar, 5μm.

(M-N, P-Q) Representative bright field (BF, top), DAPI staining (DNA, middle) and anti-activated MPK-1 staining [MPK-1(YT), bottom] images of dissected gonads from worms of indicated genotypes. Scale bar, 5μm.

(I, L, O, R) Pixel intensity quantification of anti-GLP-1 staining (I, L) or MPK-1(YT) staining (O, R) within the whole mitotic zone of worms with indicated genotypes. n= total number of gonad arms examined in each group.

Description of the approach and results. Previous studies have indicated that both the insulin and IGF (IIS) and TORC1 signaling pathways play positive roles in germ cell

proliferation, independent of GLP-1/Notch signaling (Fukuyama et al. 2006; Michaelson et al. 2010; Korta et al. 2012). Based on the phenotype alone, the impact of low U/T on mitotic proliferation of germ cells could potentially be mediated by either pathway. We have thus performed experiments to investigate the potential roles of these two pathways in germline proliferation arrest in *cdd-1/2* DKO animals.

For the IIS pathway, we hyper-activated the IIS pathway in the *cdd-1/2* DKO worms by knocking down two negative regulators downstream of the insulin receptor DAF-2, *daf-16/FOXO* and *daf-18/PTEN*, Previous reports showed that reducing *daf-16* and *daf-18* partially suppressed the germline defects caused by compromising the IIS pathway but not the TORC1 pathway (Michaelson et al. 2010; Korta et al. 2012). We found that RNAi of these genes have no effect on the proliferation arrest in the *cdd-1/2* DKO germline (A-C). Therefore, the U/T level likely acts through a pathway parallel to the IIS pathway.

For the TORC1 pathway, we used both RNAi and mutations to create constitutively activated TORC1 that had been shown to prominently suppress the robust L1 growth and developmental arrest caused by blocking lipid biosynthesis (Zhu et al. 2013). We observed no suppression of the proliferation arrest of *cdd-1/2* DKO germ cells when TORC1 was activated either by RNAi knock-down of the TORC1 inhibitor *nprl-3* or by two TORC1 activating transgenes (*daf-15::rap-1[22]* or *rheb-1[Q71L Q72D]*) (D-F).

We further analyzed the potential impact of the IIS and TORC1 pathways on the GLP-1 pathway. By immunostaining, we found that GLP-1 expression is not down regulated when either IIS or TORC1 pathways were compromised by loss-of-function mutations in the key genes of the pathways (*daf-2*/IIS pathway and *rsks-1*/TORC1 pathway) (G-I). In addition, the ectopic activation of MPK-1 we observed in the *cdd-1/2* DKO germline was not detected in the same IIS or TORC1 pathway mutants (M-R). Together with the data presented in the main text regarding the roles of the GLP-1 pathway, these data indicate that GLP-1/Notch signalling, but not IIS or TORC1 signalling, plays a pivotal role in mediating the effect of U/T level on mitotic germline proliferation.

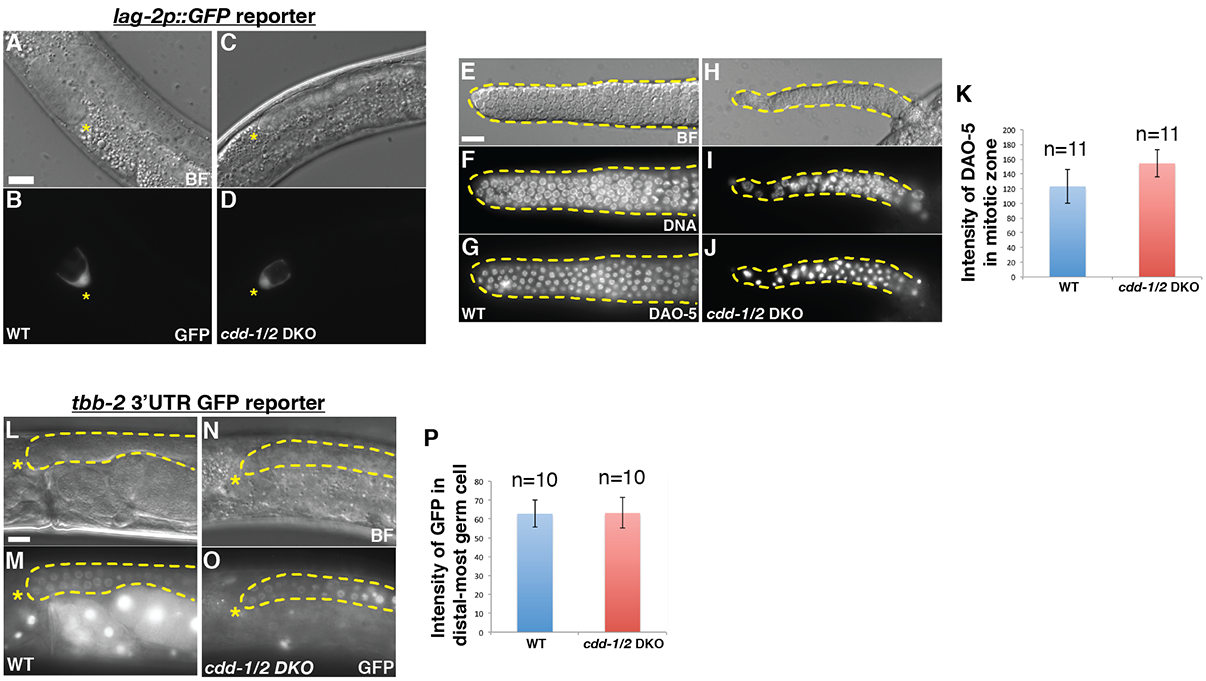

Supplemental Fig. S4, related to Fig. 4. In *cdd-1/2* DKO worms fed low U/T food, the expression of GLP-1 ligand LAG-2 is not obviously altered, and protein expression in the mitotic zone is not globally decreased.

(A-D) Representative bright field (A and C) and GFP fluorescence (B and D) images of L4 worms of indicated genotypes expressing a *lag-2p*::GFP reporter. Asterisk marks the distal end of gonad. >30 gonadal arms were examined for each genotype, all displayed similar intensity of the GFP signal. Scale bar, 20µm.

(E-J) Representative bright field (E and H), DAPI staining (F and I) and antibody staining against nucleolar marker DAO-5 (G and J) images of dissected gonads from worms of indicated genotypes. Scale bar, 5µm.

(K) Bar graphs representing the pixel intensity quantification of anti-DAO-5 staining in the mitotic zone. n=number of gonad arms examined in each group.

(L-O) Representative bright field (L and N) and GFP fluorescence (M and O) images of young adult hermaphrodites of indicated genotypes expressing a *tbb-2* 3'UTR GFP reporter. Asterisk marks the distal end of gonad; dashed line outlines germline. Scale bar, 20µm.

(P) Bar graph showing the pixel intensity quantification of GFP from individual germ cells within the distal-most germline of worms with indicated genotypes. n=number of gonad arms examined in each group.

References

Franks DM, Izumikawa T, Kitagawa H, Sugahara K, Okkema PG. 2006. C-elegans pharyngeal morphogenesis requires both de novo synthesis of pyrimidines and synthesis of heparan sulfate proteoglycans. *Dev Biol* **296**: 409-420.

Fukuyama M, Rougvie AE, Rothman JH. 2006. C. elegans DAF-18/PTEN mediates nutrient-dependent arrest of cell cycle and growth in the germline. *Current biology : CB* **16**: 773-779.

Korta DZ, Tuck S, Hubbard EJ. 2012. S6K links cell fate, cell cycle and nutrient response in C. elegans germline stem/progenitor cells. *Development* **139**: 859-870.

Michaelson D, Korta DZ, Capua Y, Hubbard EJ. 2010. Insulin signaling promotes germline proliferation in C. elegans. *Development* **137**: 671-680.

Sharan SK, Thomason LC, Kuznetsov SG, Court DL. 2009. Recombineering: a homologous recombination-based method of genetic engineering. *Nature protocols* **4**: 206-223.

Zhu H, Shen H, Sewell AK, Kniazeva M, Han M. 2013. A novel sphingolipid-TORC1 pathway critically promotes postembryonic development in Caenorhabditis elegans. *Elife* **2**: e00429.